processes

MDPI

Article

Separation of Benzene-Cyclohexane Azeotropes Via Extractive Distillation Using Deep Eutectic Solvents as Entrainers

Fang Bai [1,2,3], Chao Hua [1,3,*] and Jing Li [1,2,3]

[1] Key Laboratory of Green Process and Engineering, Institute of Process Engineering, Chinese Academy of Sciences, Beijing 100190, China; fbai@ipe.ac.cn (F.B.); lijing715@mails.ucas.ac.cn (J.L.)
[2] School of Chemical and Engineering, University of Chinese Academy of Sciences, Beijing 100049, China
[3] Innovation Academy for Green Manufacture, Chinese Academy of Sciences, Beijing 100190, China
* Correspondence: huachao@ipe.ac.cn

Abstract: The separation of benzene and cyclohexane azeotrope is one of the most challenging processes in the petrochemical industry. In this paper, deep eutectic solvents (DES) were used as solvents for the separation of benzene and cyclohexane. DES1 (1:2 mix of tetrabutylammonium bromide (TBAB) and levulinic acid (LA)), DES2 (1:2 mix of TBAB and ethylene glycol (EG)) and DES3 (1:2 mix of ChCl (choline chloride) and LA) were used as entrainers, and vapor-liquid equilibrium (VLE) measurements at atmospheric pressure revealed that a DES comprised of a 2:1 ratio of LA and TBAB could break this azeotrope with relative volatility (αij) up to 4.763. Correlation index suggested that the NRTL modelling approach fitted the experimental data very well. Mechanism of extractive distillation gained from FT-IR revealed that with hydrogen bonding and π–π bond interactions between levulinic acid and benzene could be responsible for the ability of this entrainer to break the azeotrope.

Keywords: benzene; cyclohexane; deep eutectic solvents (DES); extractive distillation; entrainer

Citation: Bai, F.; Hua, C.; Li, J. Separation of Benzene-Cyclohexane Azeotropes Via Extractive Distillation Using Deep Eutectic Solvents as Entrainers. *Processes* **2021**, *9*, 336. https://doi.org/10.3390/pr9020336

Academic Editor: Weize Wu

Received: 20 January 2021
Accepted: 5 February 2021
Published: 12 February 2021

1. Introduction

Distillation is mostly used in industry to separate liquid mixtures. However, azeotropic mixtures (or approximate boiling point systems) require special distillation processes for effective separation processes. The separation of benzene and cyclohexane azeotrope is one of the most challenging processes in the petrochemical industry. The most attractive separation technique for benzene and cyclohexane is liquid−liquid extraction [1,2]. Traditional organic solvents are usually selected as extractants, such as furfuryl alcohol, ethylene glycol, N-methyl pyrrolidone (NMP). However, these solvents are typically toxic, flammable, volatile, and difficult to recover.

In this respect, ionic liquids (ILs) have been employed as effective entrainers for separations in the fine chemical industry. However, the toxicities, low purities, and relatively high costs of these entrainers have restricted their use in the food or pharmaceutical industries. Recently, deep eutectic solvents (DESs) that contain hydrogen bond acceptor (HBA) and hydrogen bond donor (HBD) have been proposed as an alternative class of entrainer [3]. Most DESs are comprised of an organic salt as an HBA (e.g., quaternary ammonium salt, quaternary phosphine salt, etc.) and a carboxylic acid, amide, or alcohol as an HBD. However, DESs cannot contain all kinds of these solvents, and many DESs have glass transition temperatures rather than eutectic melting points. Thus, DESs are also called low transition temperature mixtures (LTTMs) [4,5]. DESs also have been studied in the field of gas-gas/liquid−liquid extraction [6–12] and extractive distillations [13–20]. Deep eutectic solvents (DESs) as novel entrainers can be used for the separation of azeotropic mixture, and have received much attention in recent years [21–23]. Shang et al. suggested that deep eutectic solvent ChCl/Urea (1:2) could be used for extractive distillation for the separation of ethanol–water [24]. The study of Samarov [25] tested Choline chloride-based deep

eutectic solvent (DES) for the separation of azeotropic mixtures of ethanol–ethyl acetate, n-propanol–n-propyl acetate and n-butanol–n-butyl acetate via liquid–liquid extraction. Some researchers believed that azeotropic phenomenon was broken because hydrogen bond sites which exist in DES have strong solvation with polar substances, thus changing the relative volatility [26–30]. However, many of these extractive processes have not been fully optimized.

In this paper, a cheap and easily prepared DES as an entrainer in benzene-cyclohexane azeotropes extractive distillation processes was reported. Vapor-liquid equilibrium (VLE) data of all DES systems were determined to evaluate the extractive distillation effect. The separation process was simulated in Aspen Plus V8.4 to select the most suitable simulation method. Furthermore, the mechanism of extractive distillation was explored by FT-IR.

2. Materials and Methods

2.1. Chemicals

All the chemicals (>98% purity) used in this study were purchased from chemical suppliers and used without further chemical purification, with choline chloride (ChCl) stored in a vacuum desiccator before use.

2.2. Preparation of DES

DES were prepared following the procedure reported in Ref [30]. Specifically, mixtures of the HBD and HBA were stirred and heated until they melted into a homogeneous liquid. Then the resultant DES was dried in a thermostatic drier box at 100 °C for 24 h. The DES were classified as DES1 (1:2 mix of tetrabutylammonium bromide (TBAB) and levulinic acid (LA)), DES2 (1:2mix of TBAB and ethylene glycol (EG)) and DES3 (1:2mix of ChCl and LA). Figure 1 showed the representative images of the DES that were prepared.

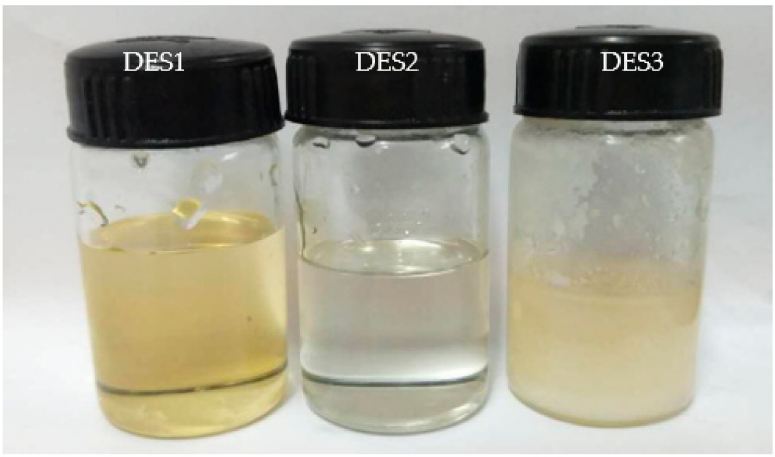

Figure 1. Experimental DES. From left to right were DES1, DES2, DES3.

2.3. Characterization of DES

The melting point and glass transition temperature of the selected DES were determined using differential scanning calorimetry (DSC) using a METTLER TOLEDO Differential Scanning Calorimeter type DSC1. All DSC experiments were carried out under a N2 atmosphere to avoid oxidation of the samples, using a N2 flow rate of 45 mL/min and a heating rate of 10 °C·min^{-1} until the sample had melted completely. The densities and viscosities of the selected DES were measured at a series of temperatures using an Anton Paar viscosity and density instrument (DMA 5000-AMVn). IR analysis was carried out using a Fourier-transformed infrared (FT-IR) spectrometer (T27-Hyperion-Vector22).

2.4. VLE Measurements

VLE measurements were conducted using an all-glass dynamic circulation vapor-liquid equilibrium still (a modified Othmer still). There was 30 mL of a liquid sample injected into an equilibrium kettle fitted with a condenser and the rate of heating adjusted until a condensation return of 2–3 drops per seconds was achieved. After refluxing for 0.5 h, the temperature was then measured every 5 min until the temperature of the distillate was constant (around 0.5 h) to ensure that the liquid and vapor phases had reached equilibrium. Next, 0.4 uL samples of the liquid and vapor phases were sampled and subjected to chromatographic analysis, with each experiment repeated three times to ensure consistency. The outlet of the condenser was maintained at ambient atmospheric pressure throughout the course of the VLE experiment. Samples were analyzed using gas chromatogram fitted with a KB-FFAP column (30 m × 0.32 mm × 0.25 um) and an FID detector using a two-stage programmed temperature method, with a slit ratio of 200. The initial column temperature was maintained at 70 °C for 1 min; then heated to 150 °C (at a rate of 15 °C·min^{-1}); maintained at 150 °C for 2 min; heated to 220 °C (at a rate of 20 °C·min^{-1}); and then maintained at 220 °C for 5 min. The oven temperature was maintained at 230 °C, the temperature of the detector was 250 °C, with high purity N_2 used as a carrier gas at a flow rate of 30 mL·min^{-1} H_2, and air flow rates of 30 mL·min^{-1} and 300 mL·min^{-1}, separately.

3. Results and Discussion

3.1. Characterization of DES

The results obtained for the melting points and glass transition temperatures of the three DES are shown in Table 1.

Table 1. Glass transition temperatures and melting points of DES.

Sample	Glass Transition Temperature (°C)	Melting Point (°C)	Melting Points of HBA Component (°C)	Melting Point of HBD Component (°C)
DES1	−70~−65	-	102~106	37.2
DES2	−52~−54	-	102~106	12.9
DES3	−72~−65	63~66	302~305	37.2

From Table 1, it can be seen that only DES1 and DES2 were found to exhibit glass transition temperatures, which occurred between 102.2–107.2 °C and 39.1–41.1 °C, which were lower than the melting points of their pure components. Furthermore, the glass transition temperature of DES1 decreased more than that of DES2, which means that the hydrogen bonding interactions in DES1 could be stronger.

The densities and viscosities measured at atmospheric pressure in duplicate from 293.15–353.15 K at temperature intervals steps of 10 K were shown in Figures 2 and 3. The relative standard deviations of the densities and the viscosities of the DES were found to be u(ρ) = 0.002 and u(u) = 0.003, respectively. The densities of DES1 and DES2 were measured at different temperatures (293.15–353.15 K) at atmospheric pressure, affording density values between 1.0~1.1 g/cm^3 that are similar to the density of water. The viscosities of DES1 and DES2 measured over the same temperature range (293.15 K~353.15 K) at atmospheric pressure decreased as the temperature increased, with their 100~1000 mPa·S viscosity values similar to those exhibited by ionic liquids. DES3 was a solid at room temperature and therefore a glass transition temperature could not be measured.

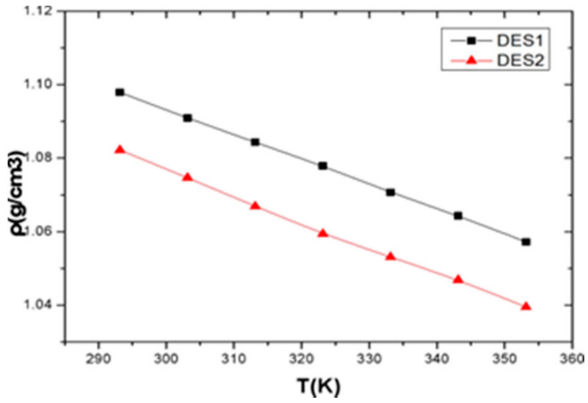

Figure 2. Variation in experimental densities of DES1 and DES2 for increasing temperature.

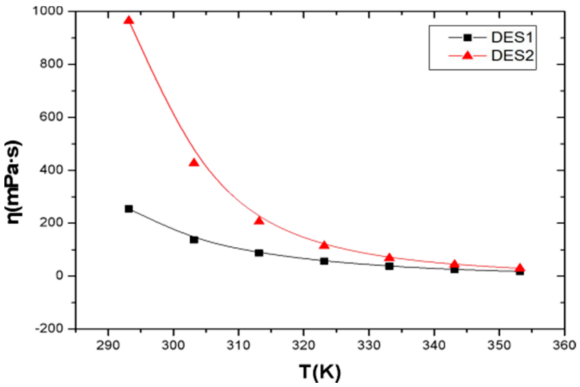

Figure 3. Variation in experimental viscosities of DES1 and DES2 for increasing temperature.

3.2. Physical Interactions between the DES

Physical interactions between the components of DES1, DES2 and DES3 were analyzed using FT-IR spectra (see Figures 4–6). As shown in Figure 4, in the infrared spectrum of LA, peaks near 3200 cm^{-1} were identified as the -OH stretching vibration peak. The peaks near 2870 cm^{-1} and near 2960 cm^{-1} were identified as the symmetric and antisymmetric stretching vibration of $–CH_3$. The peak near 2850 cm^{-1} and 2930 cm^{-1} were considered as symmetrical and anti-symmetric stretching vibration peaks stretching vibration peaks of methylene ($-CH_2-$). The peak near 1722 cm^{-1} was regarded as carbonyl group (-C=O) stretching vibration peak, and peak near 1500 cm^{-1} was identified as the antisymmetric stretching vibration peak of carboxyl group (-COO-). In the infrared spectrum of TBAB, the peaks near 2870 cm^{-1} and near 2960 cm^{-1} were identified as the symmetric and antisymmetric stretching vibration of $–CH_3$. The peak near 2850 cm^{-1} and 2930 cm^{-1} were considered as symmetrical and anti-symmetric stretching vibration peaks stretching vibration peaks of methylene ($-CH_2-$). The peak around 1200~900 cm^{-1} was regarded as stretching vibration peak of CN. As for DES1, the infrared spectrum was almost the superposition of LA and TBAB, except the hydroxyl group (-OH) near 3200 cm^{-1} that became broader and larger, red-shifted to 3000 cm^{-1}. It could be the evidence that hydrogen bonds could be formed by LA and TBAB.

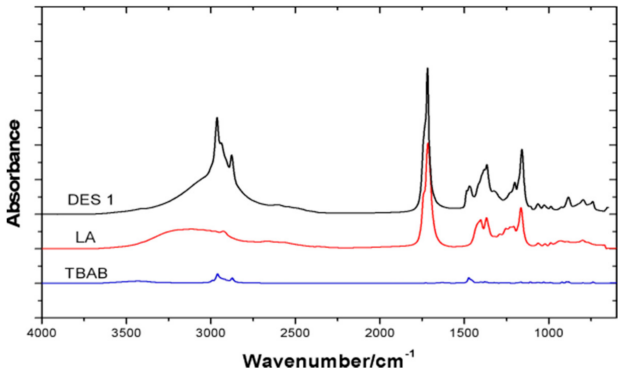

Figure 4. FT-IR spectra of TBAB, LA and DES1.

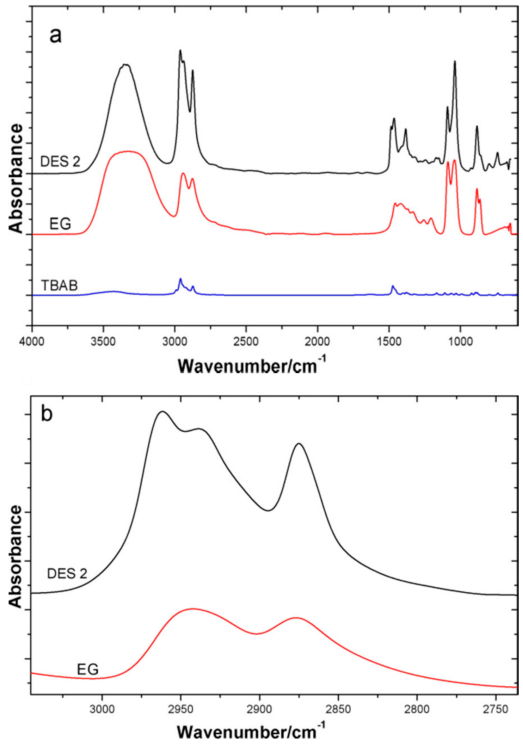

Figure 5. FT-IR spectra of TBAB, EG and DES2 ((**a**), original figure, (**b**) local amplification figure).

As shown in Figure 5a, in the infrared spectrum of EG, peaks near 3200 cm^{-1} were identified as the -OH stretching vibration peak. The peak near 2850 cm^{-1} and 2930 cm^{-1} were considered as symmetrical and anti-symmetric stretching vibration peaks stretching vibration peaks of methylene (-CH^2-). The peak around 1050~1150 cm^{-1} was regarded as stretching vibration peak of –COH. In the infrared spectrum of DES2, the red-shifted hydroxyl group (-OH) peak near 3200 cm^{-1} (shown in Figure 5b) suggested that hydrogen bonds could be formed by TBAB and EG.

As shown in Figure 6a, in the infrared spectrum of ChCl, peak near 3200 cm^{-1} were identified as the -OH stretching vibration peak. The peaks near 2870 cm^{-1} and near 2960 cm^{-1} were identified as the symmetric and antisymmetric stretching vibration of –CH_3. The peak near 2850 cm^{-1} and 2930 cm^{-1} were considered as symmetrical and anti-symmetric stretching vibration peaks stretching vibration peaks of methylene (-CH_2-). The peak around 1200~900 cm^{-1} was regarded as stretching vibration peak of CN. In the infrared spectrum of DES3, the red-shifted hydroxyl group (-OH) peak near 3200 cm^{-1} (shown in Figure 6b) suggested that hydrogen bonds could be formed by ChCl and LA.

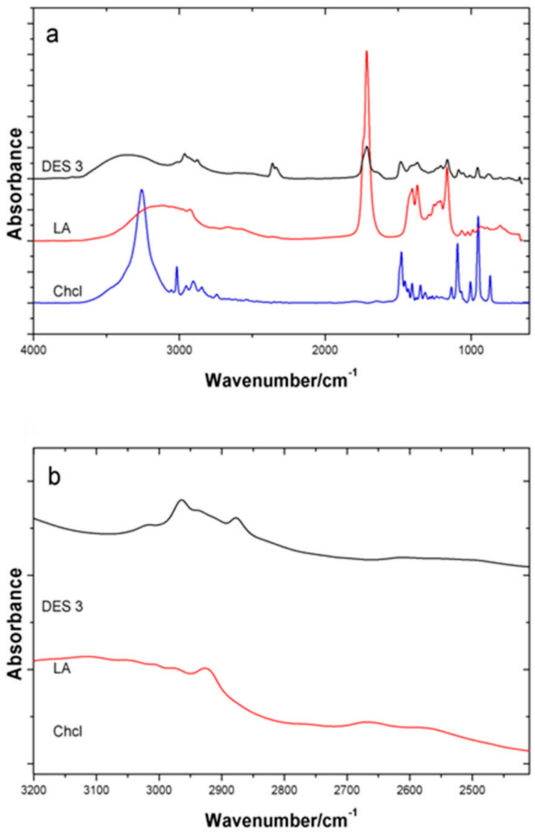

Figure 6. FT-IR spectra of ChCl, LA and DES3 ((**a**), original figure, (**b**) local amplification figure).

Therefore, hydrogen bond was proved to exist in the three DES because of active hydrogen atoms in hydrogen bond donor and high electron density of hydrogen bond acceptors.

3.3. Vapor-Liquid Equilibrium and Selection Profile of the DES

Vapor-liquid equilibrium experiment for benzene-cyclohexane-DES system was conducted experiment at atmospheric pressure. The molar concentration of extractant was 0.1. The results were listed in Table 2. Specifically, X3 is the molar fraction of low eutectic solvent in the liquid phase, X1 is the molar fraction of cyclohexane in the liquid phase at the vapor-liquid equilibrium, X'1 is the molar fraction of cyclohexane in the liquid phase at the vapor-liquid equilibrium (without DES content), Y1 is the molar fraction of cyclohexane in the gas phase at the vapor-liquid equilibrium, and T is the temperature at the vapor-liquid equilibrium. Furthermore, relative volatility (αij) and selectivity factor (S) were calculated according to the following Equations (1) and (2):

$$\alpha_{ij} = \frac{Y_i / X_i}{Y_j / X_j} \quad (1)$$

$$S = \frac{\alpha_{ij}^{\text{with entrainer}}}{\alpha_{ij}^{\text{without entrainer}}} \quad (2)$$

where, Y is the molar fraction of the vapor phase, X is the molar fraction of the liquid phase, and the subscripts i and j referred to the most volatile component (cyclohexane) and the less volatile component (benzene), respectively.

Table 2. The vapor-liquid equilibrium data of cyclohexane(1)-benzene(2)-DES(3) measured in Lab (P = 101.3 kPa).

Benzene + Cyclohexane + DES1 at 101.3 kPa						
X_3	X_1	X'_1	Y_1	T/K	α_{ij}	S
0.1	0.000	0.000	0.000	353.25	-	-
0.1	0.109	0.121	0.231	351.96	2.188	1.7398
0.1	0.167	0.185	0.319	351.20	2.060	1.7050
0.1	0.241	0.267	0.494	350.64	2.675	2.4106
0.1	0.302	0.335	0.605	351.28	3.044	3.6987
0.1	0.353	0.392	0.711	351.74	3.809	4.8978
0.1	0.451	0.501	0.809	352.34	4.223	5.7581
0.1	0.560	0.622	0.887	352.67	4.763	6.4944
0.1	0.649	0.721	0.921	352.88	4.509	6.1481
0.1	0.723	0.804	0.942	353.17	3.968	5.4104
0.1	0.900	1.000	1.000	353.85	-	-
Benzene + Cyclohexane + DES2 at 101.3 kPa						
X_3	X_1	X'_1	Y_1	T/K	α_{ij}	S
0.1	0.000	0.000	0.000	353.25	-	-
0.1	0.087	0.097	0.150	352.17	1.637	1.2526
0.1	0.111	0.123	0.184	351.91	1.607	1.2778
0.1	0.141	0.156	0.237	351.73	1.675	1.3319
0.1	0.244	0.271	0.338	351.39	1.371	1.1347
0.1	0.306	0.341	0.392	351.23	1.250	1.0346
0.1	0.434	0.482	0.496	351.03	1.056	0.9112
0.1	0.560	0.622	0.592	351.15	0.880	1.0693
0.1	0.786	0.873	0.821	352.16	0.666	0.9081
0.1	0.849	0.944	0.927	352.96	0.764	1.0417
0.1	0.900	1.000	1.000	353.85	-	-
Benzene + Cyclohexane + DES3 at 101.3 kPa						
X_3	X_1	X'_1	Y_1	T/K	α_{ij}	S
0.1	0.000	0.000	0.000	353.25	-	-
0.1	0.066	0.073	0.121	352.65	1.750	1.3390
0.1	0.127	0.141	0.181	352.15	1.344	1.0284
0.1	0.191	0.212	0.246	351.67	1.213	0.9645
0.1	0.288	0.320	0.341	351.27	1.096	0.9071
0.1	0.345	0.383	0.391	351.10	1.033	0.8914
0.1	0.438	0.487	0.481	351.17	0.977	1.1871
0.1	0.536	0.595	0.573	351.25	0.913	1.1094
0.1	0.594	0.660	0.625	351.30	0.861	1.0462
0.1	0.619	0.688	0.646	351.43	0.825	1.0608
0.1	0.705	0.783	0.737	351.95	0.775	0.9965
0.1	0.756	0.840	0.808	352.45	0.802	1.0935
0.1	0.797	0.885	0.851	352.87	0.742	1.0117
0.1	0.900	1.000	1.000	353.85	-	-

The Y1-X1 and α-X1 graphs derived from the experimental data were shown in Figures 7 and 8. As can be seen from Figure 7, when DES1 is added to the mixture system, the euboiling-point disappears. The DES2 or DES3 mixture has the same boiling point as the benzene-cyclohexane binary system. The experiment shows that DES2 and DES3 have a weak interaction with benzene and cyclohexane without changing the azeotropic point, DES1 has strong interaction with benzene or cyclohexane, which can break the azeotrope. Therefore, DES1 can be used for extractive distillation of benzene-cyclohexane.

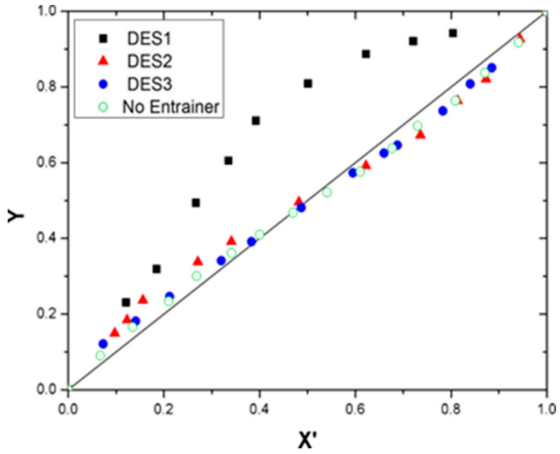

Figure 7. Experimental data for the pseudo-ternary systems (**a**) Benzene + cyclohexane + DES1; (**b**) Benzene + cyclohexane + DES2; (**c**) Benzene + cyclohexane + DES3; and (**d**) Benzene + cyclohexane.

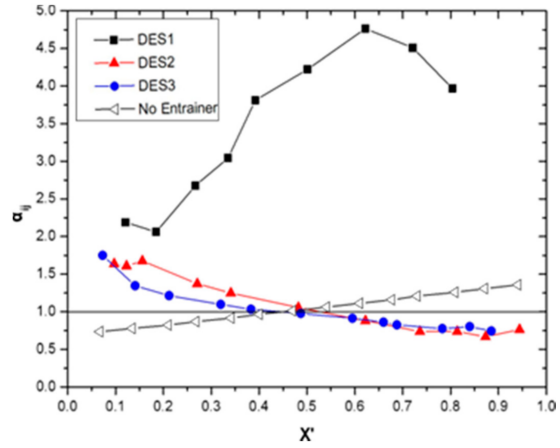

Figure 8. The X_1-α diagram of cyclohexane(1)-benzene(2)-DES(3) system at 101.3 kPa.

It is known that azeotropic point occurs when the value of the relative volatilities of the components of a distillate are equal to 1. If the azeotrope was broken, the relative volatility should be greater than 1. On the basis of Figure 8, the relative volatility was greater than 1 in the full concentration range only when extraction agent DES1 was added.

3.4. VLE Data Correlation

In this section, a continuous extraction process for separating benzene from cyclohexane was preliminarily simulated in Aspen Plus V8.4. UNIQUAC, Wilson and NRTL local composition activity coefficient models were used to fit the obtained VLE data. The correlation index R2 was calculated as the following Equation (3):

$$R^2 = 1 - \frac{\sum (y_i - u_i)^2}{\sum (y_i - \overline{y})^2} \quad (3)$$

where y_i and u_i are the experimental data and estimated values of the vapor phase molar fractions, respectively, and y is the average value of experimentally determined vapor phase molar fraction data.

From Table 3, it can be seen that coefficient of determination values (R^2) of the three systems ranked as NRTL > UNIQUAC > Wilson. The R^2 of the same model for the three systems was found to be in order of DES3 > DES2 > DES1, indicating that the model application degree of the system was changed by extractant. The better the extraction effect, the lower the model application degree.

Table 3. Related index R^2 of three thermodynamic model fitting with cyclohexane-benzene—DES system.

System	R^2		
	UNIQUAC	WILSON	NRTL
Benzene + cyclohexane + DES1	0.8232	0.6153	0.8761
Benzene + cyclohexane + DES2	0.9932	0.9932	0.9999
Benzene + cyclohexane + DES3	0.9992	0.9979	0.9995

Next, the vapor-liquid equilibrium data were simulated by NRTL model regression module, and the summary data were shown in Table 4. The phase diagram of Y_1-X_1 fitted by the cyclohexane(1)-benzene(2)-DES(3) system and the NRTL model is shown in Figures 9–11. It can be seen that the simulated data were very close to the experimental data.

Table 4. The binary interaction parameters of NRTL model fitting with cyclohexane-benzene-DES system.

Extractant	Comp.i	Comp.j	Aij	Aji	Bij	Bji	Cij
DES1	Cyclohexane	Benzene	−17.8945	26.1684	10,000	−10,000	0.1717
DES2			2.7875	13.7115	−3150.39	−2220.07	0.0170
DES3			−22.3132	181.9706	7823.07	−63,763.92	0.9320

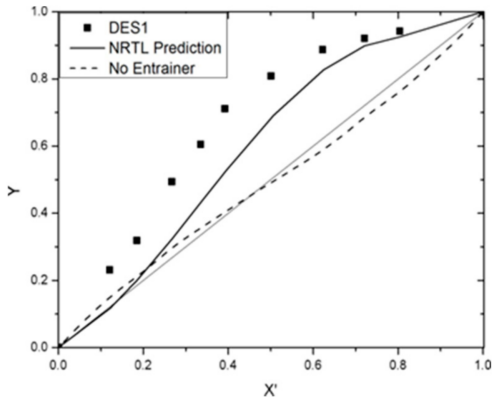

Figure 9. Experimental and simulated data for (**a**) cyclohexane, (**b**) benzene and (**c**) DES1 at 101.3 kPa for a DES molar fraction of 0.1.

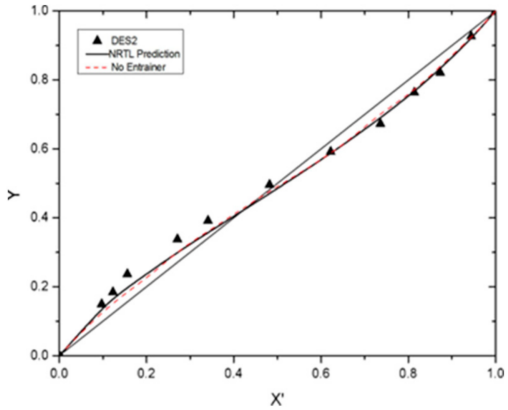

Figure 10. Experimental and simulated data for (**a**) cyclohexane, (**b**) benzene and (**c**) DES2 at 101.3 kPa for a DES molar fraction of 0.1.

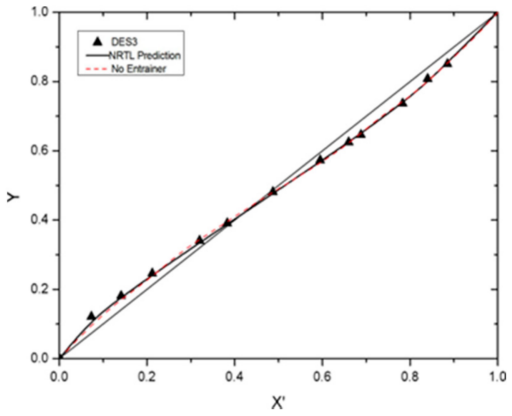

Figure 11. Experimental and simulated data for (**a**) cyclohexane, (**b**) benzene and (**c**) DES3 at 101.3 kPa for a DES molar fraction of 0.1.

3.5. Mechanism Analysis of Extractive Distillation

The mechanism of the extractive distillation process was investigated using FTIR. FT-IR spectra of DES and benzene were shown in Figures 12–14. The FT-IR spectra of DES1, DES2 and DES3 have been analyzed in Figures 4–6. In the infrared spectrum of benzene, the peak at 3030 cm^{-1} was regarded as the C-H stretching vibration peak. Peaks round 1500~1800 cm^{-1} were assigned as the benzene ring skeleton vibration peak. The peak near 1000 cm^{-1} was attributed as in-plane C-H bending vibration. As can be seen in Figure 12, compared with DES1, in the DES1 + benzene mixture, the C=O peak band near 1722 cm^{-1} became narrow, which indicates π-π bond was formed between DES1 and benzene. At the same time, the hydroxyl stretching peak band near 3200 cm^{-1} became narrowed, which indicates that the hydrogen bond between DES1 and benzene was formed, while the inner hydron bond of DES1 was broken. These results are consistent with the previous study of Hou [14], who reported that similar DES entrainers acted through π–π interactions with the aromatic ring of toluene. Due to the hydrogen bond and π-π bond between DES1 and benzene, the separation of the mixture is achieved. Conversely, comparison of the FT-IR spectra of DES2 and DES3, benzene and DES2/DES3 + benzene (see Figures 13 and 14) reveal no change in the width and intensities of their OH and C=O absorptions, which demonstrated the vapor-liquid equilibrium data.

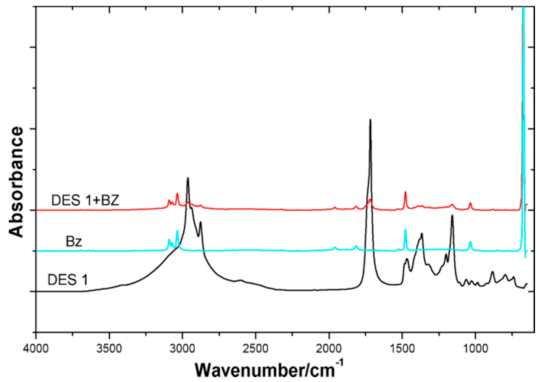

Figure 12. FT-IR spectra of (**a**) DES1 and benzene (**b**) benzene, (**c**) DES1 (DES1 = 0.1 (molar concentration)).

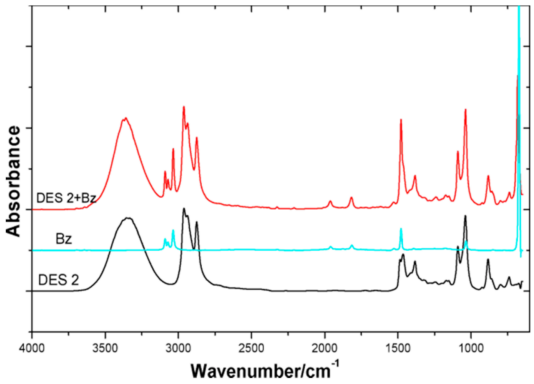

Figure 13. FT-IR spectra of (**a**) DES2 and benzene, (**b**) benzene, (**c**) DES2 (DES2 = 0.1 (molar concentration)).

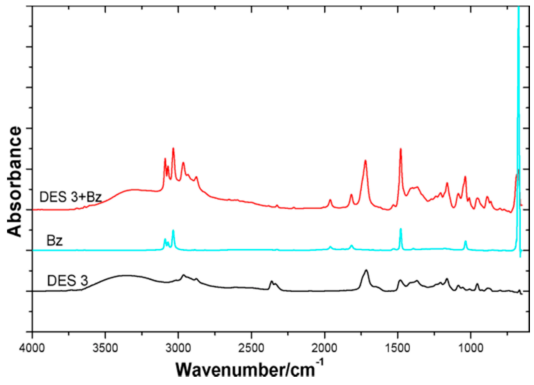

Figure 14. FT-IR spectra of (**a**) DES3 and benzene, (**b**) benzene, (**c**) DES3 (DES3 = 0.1 (molar concentration)).

4. Conclusions

In this paper, DES1 (1:2 mix of tetrabutylammonium bromide (TBAB) and levulinic acid (LA)), DES2 (1:2 mix of TBAB and ethylene glycol (EG)) and DES3 (1:2 mix of ChCl and LA) were used as entrainers for the separation of benzene and cyclohexane. Based on the VLE data of benzene−cyclohexane−DESs, DES1 has been used as an entrainer for the successful extractive distillation of azeotropic mixtures of aromatic and non-aromatic hydrocarbons. In addition, the NRTL model was applied to correlate the experimental data, and the results show that it has good agreement with the experimental data. Therefore, a continuous extraction process for separating benzene from cyclohexane was preliminarily simulated in Aspen Plus V8.4. FT-IR spectra analysis revealed that the entrainment process used to break the azeotrope relies on selective hydrogen bonding and interactions between the LA component of the DES and benzene during the distillation process. This proves that DES1 is a very promising solvent for the separation of benzene−cyclohexane mixtures.

Author Contributions: Conceptualization, F.B. and C.H.; methodology, F.B.; validation, F.B.; investigation, F.B. and J.L.; writing—original draft preparation, F.B.; writing—review and editing, F.B.; supervision, C.H. All authors have read and agreed to the published version of the manuscript.

Funding: This research was funded by The National Key Research and Development Program of China, grant number 2019YFC1907600.

Institutional Review Board Statement: Not applicable.

Informed Consent Statement: Not applicable.

Conflicts of Interest: The authors declare no conflict of interest.

References

1. Abbott, A.P.; Capper, G.; Davies, D.L.; Rasheed, R.K.; Tambyrajah, V. Novel solvent properties of choline chloride/urea mixtures. *Chem. Commun.* **2003**, 70–71. [CrossRef] [PubMed]
2. Francisco, M.; González, A.S.B.; De Dios, S.L.G.; Weggemans, W.; Kroon, M.C. Comparison of a low transition temperature mixture (LTTM) formed by lactic acid and choline chloride with choline lactate ionic liquid and the choline chloride salt: Physical properties and vapour–liquid equilibria of mixtures containing water and ethanol. *RSC Adv.* **2013**, *3*, 23553–23561. [CrossRef]
3. Durand, E.; LeComte, J.; Villeneuve, P. From green chemistry to nature: The versatile role of low transition temperature mixtures. *Biochimie* **2016**, *120*, 119–123. [CrossRef]
4. Zeng, Q.; Wang, Y.; Huang, Y.; Ding, X.; Chen, J.; Xu, K. Deep eutectic solvents as novel extraction media for protein partitioning. *Analyst* **2014**, *139*, 2565–2573. [CrossRef] [PubMed]
5. Hadi, N.A.; Ng, M.H.; Choo, Y.M.; Hashim, M.A.; Jayakumar, N.S. Performance of choline-based deep eutectic solvents in the extraction of tocols from crude palm oil. *J. Am. Oil Chem. Soc.* **2015**, *92*, 1709–1716. [CrossRef]
6. Zhang, K.; Hou, Y.; Wang, Y.; Wang, K.; Ren, S.; Wu, W. Efficient and reversible absorption of CO2 by functional deep eutectic solvents. *Energy Fuels* **2018**, *32*, 7727–7733. [CrossRef]
7. Li, N.; Wang, Y.; Xu, K.; Huang, Y.; Wen, Q.; Ding, X. Development of green Betaine-based deep eutectic solvent aqueous two-phase system for the extraction of protein. *Talanta* **2016**, *152*, 23–32. [CrossRef]
8. Gu, Y.; Hou, Y.; Ren, S.; Sun, Y.; Wu, W. Hydrophobic functional deep eutectic solvents used for efficient and reversible capture of CO_2. *ACS Omega* **2020**, *5*, 6809–6816. [CrossRef] [PubMed]
9. Paradiso, V.M.; Clemente, A.; Summo, C.; Pasqualone, A.; Caponio, F. Towards green analysis of virgin olive oil phenolic compounds: Extraction by a natural deep eutectic solvent and direct spectrophotometric detection. *Food Chem.* **2016**, *212*, 43–47. [CrossRef]
10. Qi, X.-L.; Peng, X.; Huang, Y.-Y.; Li, L.; Wei, Z.-F.; Zu, Y.; Fu, Y.-J. Green and efficient extraction of bioactive flavonoids from Equisetum palustre L. by deep eutectic solvents-based negative pressure cavitation method combined with macroporous resin enrichment. *Ind. Crops Prod.* **2015**, *70*, 142–148. [CrossRef]
11. Wei, Z.-F.; Wang, X.-Q.; Peng, X.; Wang, W.; Zhao, C.; Zu, Y.; Fu, Y.-J. Fast and green extraction and separation of main bioactive flavonoids from Radix Scutellariae. *Ind. Crops Prod.* **2015**, *63*, 175–181. [CrossRef]
12. Gonzalez, A.S.B.; Francisco, M.; de Dios, S.L.G.; Kroon, M.C. Liquid-liquid equilibrium data for the systems {LTTM plus benzene plus hexane} and {LTTM plus ethyl acetate plus hexane} at different temperatures and atmospheric pressure. *Fluid Phase Equilib.* **2013**, *360*, 54–62. [CrossRef]
13. Zhang, H.; Tang, B.; Row, K. Extraction of catechin compounds from green tea with a new green solvent. *Chem Res. Chin. Univ.* **2014**, *30*, 37–41. [CrossRef]
14. Hou, Y.; Li, Z.; Ren, S.; Wu, W. Separation of toluene from toluene/alkane mixtures with phosphonium salt based deep eutectic solvents. *Fuel Process. Technol.* **2015**, *135*, 99–104. [CrossRef]
15. Jiao, T.; Zhuang, X.; He, H.; Li, C.; Chen, H.; Zhang, S. Separation of phenolic compounds from coal tar via liquid–liquid extraction using amide compounds. *Ind. Eng. Chem. Res.* **2015**, *54*, 2573–2579. [CrossRef]
16. Yao, C.F.; Hou, Y.C.; Sun, Y.; Wu, W.Z.; Ren, S.H.; Liu, H. Extraction of aromatics from aliphatics using a hydrophobic dica-tionic ionic liquid adjusted with small-content water. *Sep. Purif. Technol.* **2020**, *236*, 116287. [CrossRef]
17. Kareem, M.A.; Mjalli, F.S.; Hashim, M.A.; Hadj-Kali, M.K.; Bagh, F.S.G.; Alnashef, I.M. Phase equilibria of toluene/heptane with tetrabutylphosphonium bromide based deep eutectic solvents for the potential use in the separation of aromatics from naphtha. *Fluid Phase Equilib.* **2012**, *333*, 47–54. [CrossRef]
18. Maugeri, Z.; Leitner, W.; De Maria, P.D. Practical separation of alcohol–ester mixtures using Deep-Eutectic-Solvents. *Tetrahedron Lett.* **2012**, *53*, 6968–6971. [CrossRef]
19. Oliveira, F.S.; Pereiro, A.B.; Rebelo, L.P.N.; Marrucho, I.M. Deep eutectic solvents as extraction media for azeotropic mixtures. *Green Chem.* **2013**, *15*, 1326–1330. [CrossRef]
20. Hizaddin, H.F.; Hadj-Kali, M.K.; Ramalingam, A.; Hashim, M.A. Extraction of nitrogen compounds from diesel fuel using imidazolium- and pyridinium-based ionic liquids: Experiments, COSMO-RS prediction and NRTL correlation. *Fluid Phase Equilib.* **2015**, *405*, 55–67. [CrossRef]
21. Peng, Y.; Lu, X.; Liu, B.; Zhu, J. Separation of azeotropic mixtures (ethanol and water) enhanced by deep eutectic solvents. *Fluid Phase Equilib.* **2017**, *448*, 128–134. [CrossRef]
22. Pan, Q.; Shang, X.; Li, J.; Ma, S.; Li, L.; Sun, L. Energy-efficient separation process and control scheme for extractive distillation of ethanol-water using deep eutectic solvent. *Sep. Purif. Technol.* **2019**, *219*, 113–126. [CrossRef]
23. Sharma, B.; Singh, N.; Kushwaha, J.P. Ammonium-based deep eutectic solvent as entrainer for separation of acetonitrile–water mixture by extractive distillation. *J. Mol. Liq.* **2019**, *285*, 185–193. [CrossRef]
24. Shang, X.; Ma, S.; Pan, Q.; Li, J.; Sun, Y.; Ji, K.; Sun, L. Process analysis of extractive distillation for the separation of ethanol–water using deep eutectic solvent as entrainer. *Chem. Eng. Res. Des.* **2019**, *148*, 298–311. [CrossRef]
25. Toikka, M.; Smirnov, M.A.; Toikka, A.M.; Prikhodko, I.V. Study of deep eutectic solvent on the base choline chloride as entrainer for the separation alcohol–ester systems. *J. Chem. Eng. Data* **2018**, *63*, 1877–1884. [CrossRef]
26. Li, C.; Zhang, J.; Li, Z.; Yin, J.; Cui, Y.; Liu, Y.; Yang, G. Extraction desulfurization of fuels with 'metal ions' based deep eutectic solvents (MDESs). *Green Chem.* **2016**, *18*, 3789–3795. [CrossRef]

27. Rodriguez, N.R.; Kroon, M.C. Isopropanol dehydration via extractive distillation using low transition temperature mixtures as entrainers. *J. Chem. Thermodyn.* **2015**, *85*, 216–221. [CrossRef]
28. Gjineci, N.; Boli, E.; Tzani, A.; Detsi, A.; Voutsas, E. Separation of the ethanol/water azeotropic mixture using ionic liquids and deep eutectic solvents. *Fluid Phase Equilib.* **2016**, *424*, 1–7. [CrossRef]
29. Abbott, A.P.; Boothby, D.; Capper, G.; Davies, D.L.; Rasheed, R.K. Deep eutectic solvents formed between choline chloride and carboxylic acids: Versatile alternatives to ionic liquids. *J. Am. Chem. Soc.* **2004**, *126*, 9142–9147. [CrossRef]
30. Mi, W.; Tong, R.; Hua, C.; Yue, K.; Jia, D.; Lu, P.; Bai, F. Vapor–liquid equilibrium data for binary systems of n,n-dimethylacetamide with cyclohexene, cyclohexane, and benzene separately at atmospheric pressure. *J. Chem. Eng. Data* **2015**, *60*, 3063–3068. [CrossRef]